INFLUENCES OF LAMINATE PARAMETERS ON THE INDUCTION HEATING BEHAVIOR OF CFRPC

Stephan Becker[1], Peter Mitschang[1]

[1]Institut für Verbundwerkstoffe GmbH, Manufacturing Science, Erwin-Schrödinger-Str. Geb. 58, 67663 Kaiserslautern, Germany
Email: stephan.becker@ivw.uni-kl.de, Web Page: http:// www.ivw.uni-kl.de
Email: peter.mitschang@ivw.uni-kl.de, Web Page: http:// www.ivw.uni-kl.de

Keywords: induction heating, heating rate, temperature distribution, fiber volume content

Abstract

Induction heating provides a fast and contactless heating of thermoplastic carbon fiber reinforced polymer composites (CFRPC) and helps to make welding processes more efficient. Within this study the influences of fiber volume content (FVC) on the inductive heating behavior of thermoplastic CFRPC is assessed. Therefore, stationary heating experiments with specimens differing in CF reinforement textile and FVC were carried out. By comparing the heating rates of the induction coil faced and opposite surface, the influences of the FVC can be identified. It was found that a higher FVC promotes a linear increase of heating rate of CFRPC by means of induction heating. Additionally, the increase of heating rate depends on the CF fabric and the contact area between differently orientated CF rovings. The lower the number of crossovers in the textile the higher is the slope of the heating rate as function of FVC within the range of this study. These results are also confirmed by microsections of the specimens.

1. Introduction

By means of the induction heating technology, eddy currents can be induced into carbon fiber reinforced polymer composite (CFRPC) laminates since the carbon fiber (CF) is electricallyconductible [1]. These eddy currents cause an intrinsic and contactless heating of CFRPC parts due to three mechanisms. Due to the fiber’s electrical resistance which is determined by their resistivity, length and cross-sectional area, heat is generated within the fiber if eddy currents run through it. This heating mechanism is also known as Joule losses. The other two heating mechanism occurs between fiber-fiber cross junctions. The junction heating mechanism describes the heat generation due to the contact resistance between two fibers. If two fibers are separated by a thin layer of a dielectrical matrix, heating by dielectric hysteresis occurs. The matrix behaves as capacitor and resistor, which are connected in a parallel circuit. In order to improve the efficiency of the induction heating technology for thermoplastic CFRPC, it is necessary to determine and understand the physical fundamentals of induction heating of CFRPC. Although the influences of the textile parameters on the inductive heating behavior has already been determined in [2], further laminate parameters have also to be investigated. Within this study the influence of the FVC was investigated by means of inductive heating experiments.

2. Materials

In order to cover a larger range of validity the manufactured specimens differ also in the (CF) reinforcement (Table 1). Thus, the specimens made of three different weave styles (twill, plain and satin) and one non-crimped fabric (NFC). In order to easily differentiate the results, the specimens were summarized in five groups. These groups are named for the used CF textile and its nominal area weight. Since the satin was not available with an nominal area weight of 200 g/m^2, the comparison of satin and twill was done with an nominal area weight of 290 g/m² and 285 g/m^2 respectively. In order to determine the effective area weight of each fabric a stack with a defined number of fabric layers and a defined area was weighed. Thus, the mean weight of a single fabric layer and consequently the effective area weight was calculated. Table 1 summerizes the textile characteristics, effective area weight, thread count, linear mass, and number of crossovers. All fabrics consists of rovings with a linear density of ρ_{lin} = 200 tex. The fabrics with a nominal area density of m_{a} = 200 g/m^2 have a thread-count of c = 5 threads/cm. Due to the higher thread-count of c = 7 threads/cm the satin as well as the second twill fabric provide a higher area weight.

Table 1. Type of reinforcements and polymer used within this study

Name of the specimen group	NCF 200	Plain 200	Twill 200	Twill 285	Satin 290
Reinforcement textile	NCF ±45°	Plain	Twill 2/2	Twill 2/2	Satin 1/4
Effective area weight $m_{\text{a,eff}}$ in g/m^2	200	201	200	276	285
Thread-count c in threads/cm	5	5	5	7	7
Linear mass density ρ_{lin} in tex	200	200	200	200	200
Number of crossovers per cm^2	0	13	6,5	12	11
Polymer	PA66	PA66	PA66	PA66	PA66

According to the data sheet the melting temperature range of the used PA66 is at T_{m} = 258-260 °C. The PA66 films are provided at thickness of 100 µm and 150 µm respectively. For each kind of CF fabric specimens with a desired FVC of φ = 30%, φ = 45% and φ = 60% and desired laminate thickness of $h_{lam.,des}$ = 2.2 mm are manufactured. . By means of the number of CF layers n, the density of the CF ρ_{CF} = 1,78 g/cm^2, the effective area weight $m_{\text{a,eff}}$ and laminate thickness h_{lam}, the corresponding FVC φ can be calculated (Eq. 1).

$$\varphi = \frac{n * m_{\text{a,eff}}}{\rho_{\text{CF}} * h_{\text{lam}}} \tag{1}$$

In addition the fixed thickness of the polymer film has to be taken into account and restricts the achievable laminate thickness. Due to the discrete number of PA66 films and the desired FVC a new target laminate thickness is provided. Table 2 shows the calculated individual laminate thickness and FVC for each fiber polymer combination.

All specimens were produced by film-stacking in an autoclave (maximum temperature of 280 °C, holdingtime 10 min, pressure 2.4 MPa during complete processing). One sheet for each parameter variation was produced in the dimensions 400 mm x 150 mm. Four specimens were cut out of each sheet with the measurement 150 mm x 100 mm. Before the experiments were carried out all specimens were dried in an oven at 90 °C for 12 h.

Table 2. Derivation of the individual laminate thickness and effective FVC. Messured laminate thickness and calculated FVC of specimens

	Desired FVC φ_{desire}	Number of CF layers n	Total thickness of PA66 films h_{PA66}, in mm	Calculated thickness of the laminate in mm	Targeted FVC φ_{target}	Measured laminate thickness h_{lam} in mm	Calculated FVC φ_{lam}
NCF 200	30%	6	1.55	2.22	30.2%	2.16	31.26%
	45%	9	1.20	2.21	45.7%	2.23	45.35%
	60%	12	0.90	2.25	60.0%	2.37	57.04%
Plain 200	30%	6	1.55	2.23	30.5%	2.11	32.05%
	45%	9	1.20	2.22	45.9%	2.33	43.62%
	60%	12	0.90	2.26	60.2%	2.44	55.54%
Twill 200	30%	6	1.55	2.22	30.2%	2.24	30.08%
	45%	9	1.20	2.21	45.7%	2.32	43.64%
	60%	12	0.90	2.25	60.0%	2.53	53.30%
Twill 285	30%	4	1.50	2.12	29.2%	2.13	29.26%
	45%	6	1.20	2.13	43.7%	2.15	43.47%
	60%	8	0.90	2.14	57.9%	2.22	57.69%
Satin 290	30%	4	1.50	2.14	29.9%	2.12	30.14%
	45%	6	1.20	2.16	44.4%	2.14	44.79%
	60%	8	0.90	2.18	58.7%	2.15	57.83%

3. Experimental Set-up

Within the heating experiments the laminates were fixed in a vertical position and heated in the center with a circular pancake coil (Ø25 mm) as described in detail in [2] (Figure 1). The used induction generator Power Cube PW3-32/400 from CEIA was operated with a constant power of 40 %. The maximum temperatures of both surfaces of the laminate were measured and recorded by means of two TIM 160 infrared cameras from MICRO-EPSILON with a field of view of 48°. Both infrared cameras are measuring simultaneously and connected to a YOKOGAWA recorder GP20. Hence, the measurement of the heating curves starts automatically once the induction generator starts to operate. A maximum temperature of 180 °C on the induction coil faced surface was chosen as stop criterion to prevent deconsolidation and phase change of the CF/PA66 laminate.

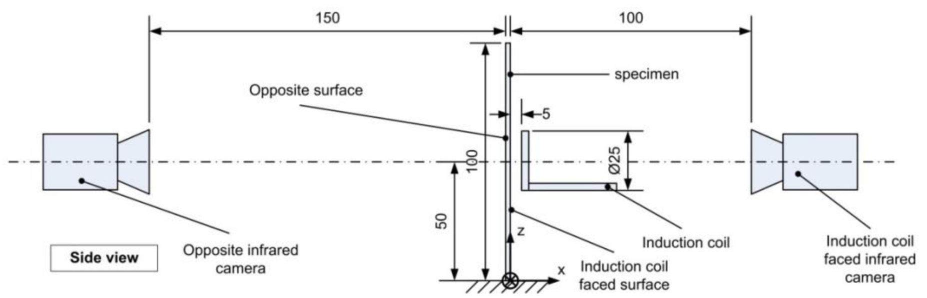

Figure 1. Schematic depiction of the experimental set-up for the heating experiments [2].

Since the surface conditions of the specimens were different, also the emissivity of each specimen differs. In order to exclude an observational error an emissivity tape (ET) with an emissivity of 0.95 was applied on both surfaces of all specimens. It is proved that the influence of the ET on the inductive heating behavior does not affect the validity of the results [2].

4. Methods

Before the experiments were carried out the laminate thickness of all specimens were measured by means of a digital caliper with a resolution of 0.01 mm. In order to determine the FVC all specimens were weighed. Since the number of layers, the effective area weight of the fabrics, the mass density of CF and the laminate thicnkness are known, the FVC of the laminates can be calculated.

During heating experiments for each time interval Δt a temperature value of each surface is recorded (Eq. 2). T_{i} indicates the temperatures measured on the induction coil faced surface, T_{o} indicates the temperatures measured on the opposite surface. The index k is set for the time interval when the measured temperature exeeds for the first time the maximum allowed temperature of 180 °C. Postprocessing is performed in a time range from $t = 0$ to $t = t_{k\text{-}1}\cdot$(time interval). Based on these values the heating rate between each specimen surface was calculated and compared. The first measured value of the opposite surface $T_{\mathrm{o},1}$ represents the ambient temperature and consequently the initial temperature of the laminate. Due to the temperature of the cooling liquid the induction coil has an initial temperature of approximately $T_{\mathrm{i},1} \approx 32$ °C, which is measured by the infrared camera. This failure is corrected by using the opposite surface temperature also as initial temperature of the induction coil faced surface.

$$\begin{pmatrix} t \\ T_{\mathrm{i}} \\ T_{\mathrm{o}} \end{pmatrix} = \begin{pmatrix} 0{,}0\,\mathrm{s} & 0{,}1\,\mathrm{s} & 0{,}2\,\mathrm{s} & \dots & t_{k\text{-}5} & t_{k\text{-}4} & t_{k\text{-}3} & t_{k\text{-}2} & t_{k\text{-}1} & t_{k} \\ T_{\mathrm{i},1} & T_{\mathrm{i},2} & T_{\mathrm{i},3} & \dots & T_{\mathrm{i},k\text{-}5} & T_{\mathrm{i},k\text{-}4} & T_{\mathrm{i},k\text{-}3} & T_{\mathrm{i},k\text{-}2} & T_{\mathrm{i},k\text{-}1} & T_{\mathrm{i},k} \\ T_{\mathrm{o},1} & T_{\mathrm{o},2} & T_{\mathrm{o},3} & \dots & T_{\mathrm{o},k\text{-}5} & T_{\mathrm{o},k\text{-}4} & T_{\mathrm{o},k\text{-}3} & T_{\mathrm{o},k\text{-}2} & T_{\mathrm{o},k\text{-}1} & T_{\mathrm{o},k} \end{pmatrix} \tag{2}$$

To exclude single outliers the representive heating rate of the induction coil faced surface $\dot{T}_{\mathrm{i}}$ is calculated by determining the average secant slope between the initial temperature $T_{\mathrm{o},1}$ and the five last measure values below 180 °C ($T_{\mathrm{i},k\text{-}5}$, $T_{\mathrm{i},k\text{-}4}$, $T_{\mathrm{i},k\text{-}3}$, $T_{\mathrm{i},k\text{-}2}$, $T_{\mathrm{i},k\text{-}1}$) of all four specimens at a certain FVC (Eq. 3).

$$\dot{T}_{\mathrm{i}} = \frac{\frac{T_{\mathrm{i},k-1} - T_{\mathrm{o},1}}{t_{k-1}} + \frac{T_{\mathrm{i},k-2} - T_{\mathrm{o},1}}{t_{k-2}} + \frac{T_{\mathrm{i},k-3} - T_{\mathrm{o},1}}{t_{k-3}} + \frac{T_{\mathrm{i},k-4} - T_{\mathrm{o},1}}{t_{k-4}} + \frac{T_{\mathrm{i},k-5} - T_{\mathrm{o},1}}{t_{k-5}}}{5} = {}^{1}\!/_{5} \sum_{g=1}^{5} \frac{T_{\mathrm{i},k-\mathrm{g}} - T_{\mathrm{o},1}}{t_{k-g}} \tag{3}$$

To determine the representive heating rate of the opposite surface $\dot{T}_{\mathrm{o}}$, the same time range as for calculating $\dot{T}_{\mathrm{i}}$ was used (Eq. 4). Since the heating graph is quite linear this approach seems to be correct (Figure 2).

$$\dot{T}_{\mathrm{o}} = \frac{\frac{T_{\mathrm{o},k-1} - T_{\mathrm{o},1}}{t_{k-1}} + \frac{T_{\mathrm{o},k-2} - T_{\mathrm{o},1}}{t_{k-2}} + \frac{T_{\mathrm{o},k-3} - T_{\mathrm{o},1}}{t_{k-3}} + \frac{T_{\mathrm{o},k-4} - T_{\mathrm{o},1}}{t_{k-4}} + \frac{T_{\mathrm{o},k-5} - T_{\mathrm{o},1}}{t_{k-5}}}{5} = {}^{1}\!/_{5} \sum_{g=1}^{5} \frac{T_{\mathrm{o},k-\mathrm{g}} - T_{\mathrm{o},1}}{t_{k-g}} \tag{4}$$

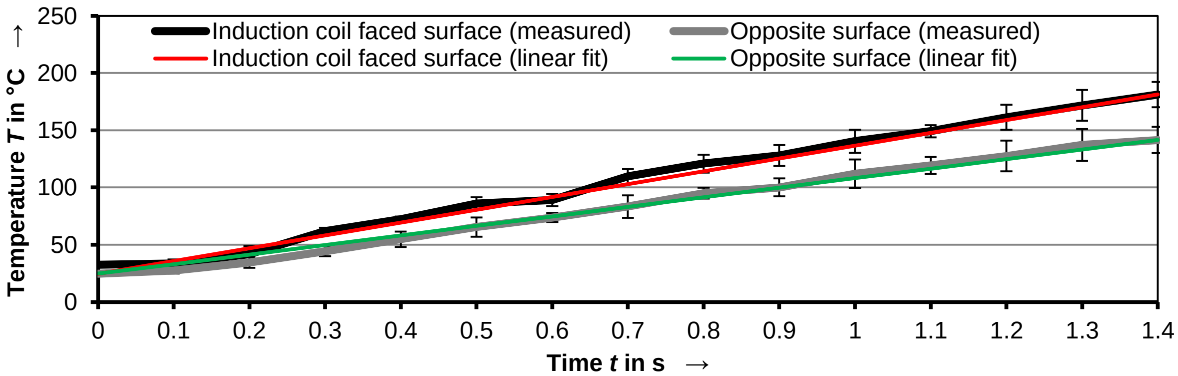

Figure 2. Comparison of the measured temperatures and the linear fittings for NCF 200 specimens with a FVC of φ = 60%. .

5. Results and Discussion

Plain 200 with a FVC of $\varphi = 30\%$ has the smallest laminate thickness with $h_{\mathrm{lam}} = 2.11$ mm. The highest laminate thickness has Twill 200 with a FVC of $\varphi = 60\%$ with $h_{\mathrm{lam}} = 2.53$ mm (Table 2). The higher measured laminate thickness compared to the calculated laminate thickness is caused by voids, which are contained in the laminate. NCF 200, Plain 200 and Twill 200 meet the targeted laminate thickness at a FVC of $\varphi = 30\%$ quite well. However, the difference between measured and targeted laminate thickness increase with the FVC. The divergence of the laminate thicknesses only slightly effects the achieved FVC.

The resulted void content can be determined through the ratio of the real laminate thickness to the targeted laminate thickness (Table 3). If the ratio is positive, this value represents the void content of the laminate. If this value is negative, the content of polymer within the laminate is too low and consequently the real FVC will be higher than the targeted FVC. Indeed, these two effects occurs at the same time.

Table 3. Ratio of target laminate thickness to measured laminate thickness

	NCF 200			Plain 200			Twill 200			Twil 285			Twill 290		
	30%	**45%**	**60%**	**30%**	**45%**	**60%**	**30%**	**45%**	**60%**	**30%**	**45%**	**60%**	**30%**	**45%**	**60%**
Ratio of target laminate thickness to measured laminate thickness	-2.87%	0.90%	4.86%	-5.54%	4.64%	7.30%	1.03%	4.66%	11.07%	0.24%	0.70%	3.39%	-0.80%	-0.79%	-1.25%
FVC of the laminate	31.26%	45.35%	57.04%	32.05%	43.62%	55.54%	30.08%	43.64%	53.30%	29.26%	43.47%	57.69%	30.14%	44.79%	57.83%

Figure 3 shows the comparison of the heating rates of all samples. As a first result one can see that the higher the FVC the higher the heating rate. As already found for different textile parameters [2], lower heating rates provide a smaller standard deviation as well as lower difference between the heating rates of both laminate surfaces. The same results can be noted within this study. Second, it can be noted that the increase of the heating rate is linear to the increase of the FVC within the range of this study. Through a linear best fitting approach linear equations for the heating rate in relation to the FVC can be determined. The linear fitting approach yields quite good coefficients of determination, which are very close to the value 1. In order to discuss the tendencies of the inductive heating behavior the slope and the *y*-intercept of the linear fits are compared (Table 4 and Table 5). In order to evaluate the influence of the area weight and consequently of the number of layers, the specimens were separated in two groups.

The intensity of the increase of the heating rate due to an increase of the FVC is described by the slope of the best fit line. Hence, the magnitude of the slope represents the influence of the laminate compaction. Consequently, the compaction forces applied on the fabric layers is higher for higher FVC. Thus, the already existed contact area between crossing rovings (threads) will be enlarged and addtional areas of contact will emerge within one layer as well as between layers. Through larger contact areas the inductive heating will be enhanced due to better contact resistance and dielectric hysterises conditions. If the magnitude of the slope is high – like the slope of NCF 200 – the resultant heating rate is strongly dependent by the FVC. In the case of the NCF 200 a higher FVC leads to a stronger increase of contact area than in the case of the Plain 200. The lower the number of crossover the higher is the slope within the range of this study.

The *y*-intercept is also a characteristic quantity and describes the extent of the contact area within a fabric layer if no compaction force is applied. The weave style Plain 200 provides a higher *y*-intercept compared to Twill 200. The lowest *y*-intercept provides NCF 200, because there is a minor contact area between the different orientated CF in a layer if no compaction force is applied. This corresponds to the fabric ranking regarding the in-plane crossovers (Table 1). The higher the number of crossover the higher is the *y*-intercept.

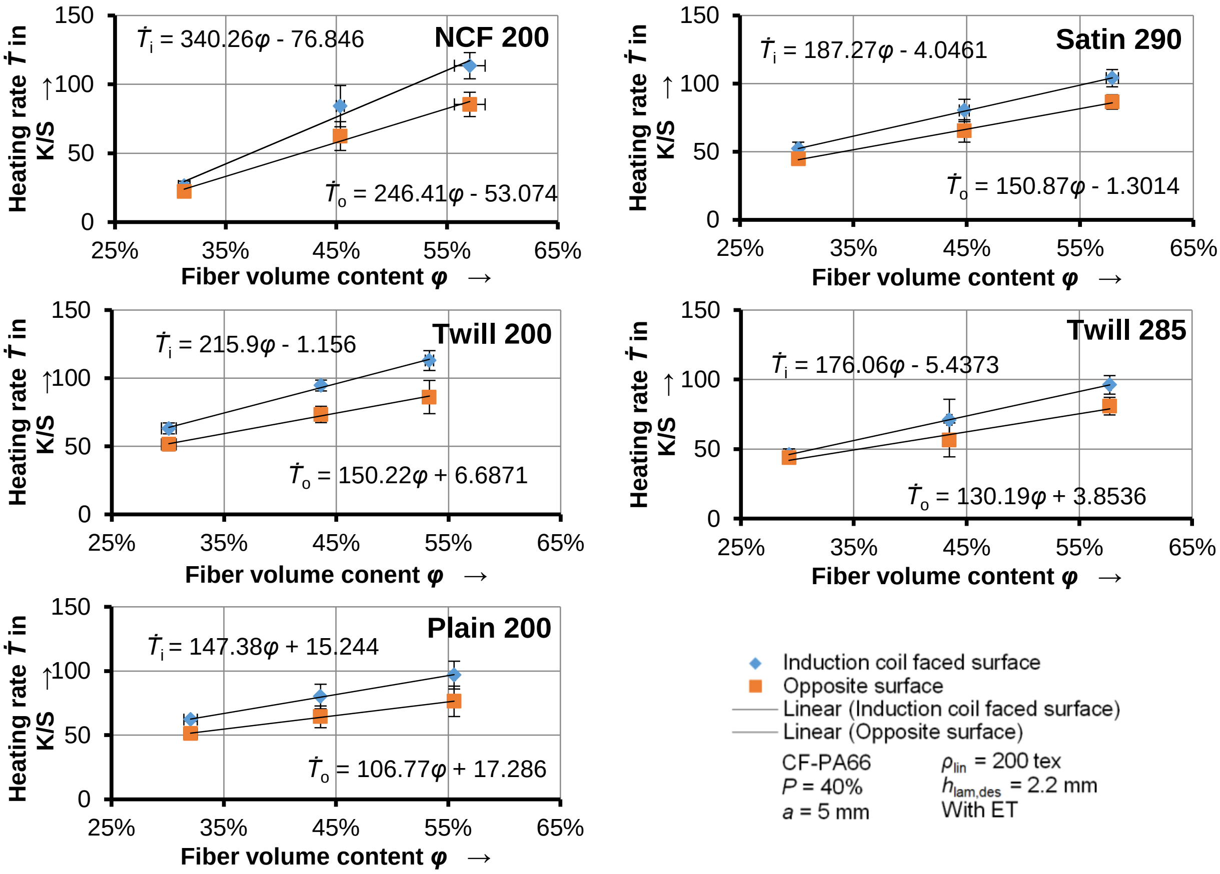

Figure 3. Heating rates of the specimens in relation to the real FVC and line of best fit. The zero values are suppressed at all x-axis.

Table 4. Heating rate on the induction coil faced surface regarding the different CF fabric.

Name of the specimen group	CF fabric	Effective area weight	Thread-count *c* threads/cm	Number of crossover per cm²	Slope *s* in K/s	*y*-intercept $\dot{T}_0$ in K/s	coefficient of determination
Plain 200	Plain	200	5	13	147.38	15.244	0.9992
Twill 200	Twill	201	5	6,5	215.90	-1.156	0.9969
NCF 200	NCF	200	5	0	340.26	-76.846	0.9822
Twill 285	Twill	276	7	12	176.06	-5,4373	0.9999
Satin 290	Satin	285	7	11	187.27	-4.0461	0.9998

Table 5. Heating rate on the opposite surface regarding the different CF fabric.

Name of the specimen group	CF fabric	Effective area weight	Thread-count *c* threads/cm	Number of crossover per cm²	Slope *s* in K/s	*y*-intercept $\dot{T}_0$ in K/s	coefficient of determination
Plain 200	Plain	200	5	13	106.77	17.286	0.9987
Twill 200	Twill	201	5	6,5	150.22	6.6871	0.9970
NCF 200	NCF	200	5	0	246.41	-53.074	0.9895
Twill 285	Twill	276	7	12	130.19	3.8536	0.9684
Satin 290	Satin	285	7	11	150.87	-1.3014	0.9981

Considering these two effects gives an explanation for the fact that the heating rates of NCF 200 at $\varphi = 30$ % are lower than the heating rate of Twill 200 and Plain 200 at the same FVC, but at a FVC of $\varphi = 60$ % NCF 200 provides the highest heating rate of all specimens. At a low FVC NCF 200 provides a minor contact area which leads to a low heating rate. Due to the increase of the FVC the necessary compaction force will increase and the contact area in total increases, too. The microsections confirm the gained results (Table 6).

Table 6. Microsections of the specimens group in relation to their FVC.

	φ = 30%	φ = 60%
Plain 200	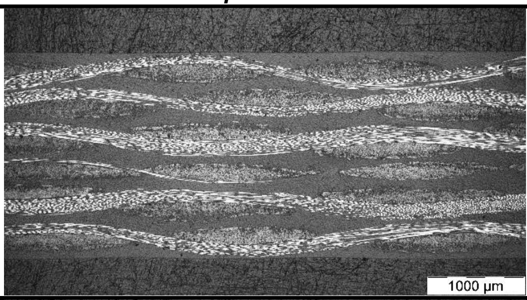	
Twill 200	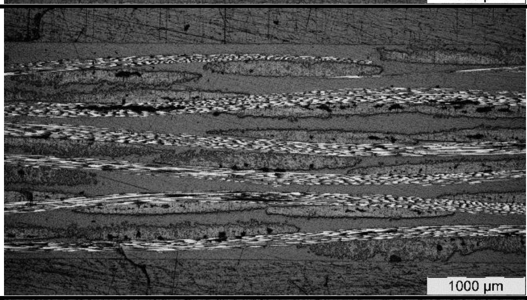	
NCF 200		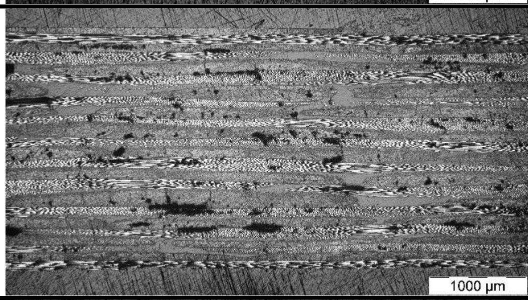
Twill 285	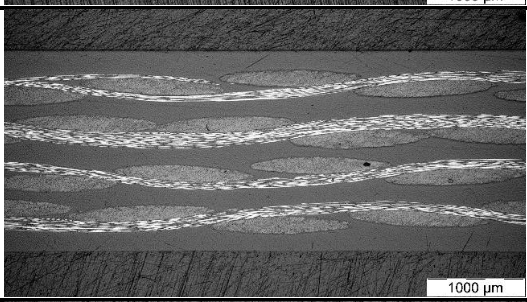	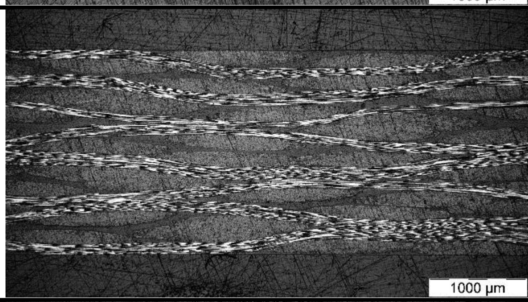
Satin 290	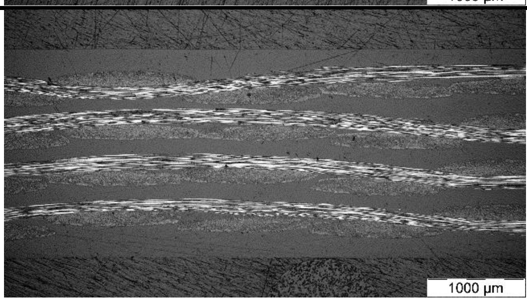	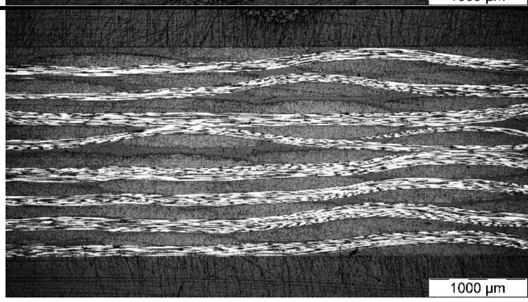

At a FVC of $\varphi = 30\%$ the resultant contact area at fiber-fiber junctions only occurs between the different orientated CF within a layer. The layers are separated through matrix rich layers. Once the FVC increases with higher compaction forces the thickness of the matrix rich layers will be reduced until the adjacent layer get in contact. Since the knitting yarn of the NCF consists of polyester (PES), which melts at 240-260 °C, the single plies of a layer can move freely during the autoclave process.

Matrix rich layers will be reduced due to an increase of the FVC. Consequently, the contact area will increase in-plane and out-of-plane much stronger then compared to weave fabrics.

Comparing Twill 200 and the Twill 285, it can be noted that an increase of the thread-count involves a reduction of the slope and of the *y*-intercept on both surfaces. The smaller slope can be explained through the higher area weight which evokes from the higher thread-count. Due to the higher area weight a layer comprises more CF material and less layers are necessary to achieve a certain FVC. Therefore, the influence of the FVC on the resultant contact area especially between single layers is smaller. The reduction of the *y*-intercept is based on the lower width of a roving which is a result of a higher thread-count. Due to the lower width of the roving the resultant contact area is smaller compared to laminate with a lower thread-count. This plays also a role if no compaction force is applied.

Comparing the two CF fabrics with a thread-count of $c = 7$ threads/cm it can be noted that the difference of the *y*-intercepts as well as of the slopes, respectively, are quite small. Comparing the crossovers, both fabrics show similar values. In order to provide the same heating behavior the resultant contact area have to be the same. The number of crossovers seems to by a major indicator to compare the influence of different weave styles.

6. Conclusions

Within this study the influences of the FVC was investigated. Therefore, specimens which differ in CF fabric and in FVC were manufactured. In order to ensure the validity of the specimens' quality, the thickness and the FVC of the specimens were determined. By means of static heating experiments the temperature on the induction coil faced and opposite surface was measured. Based on these results heating rates were calculated to compare the influence of the FVC and the different CF fabrics. The comparison showed that an increase of the FVC lead to a higher heating rate. This dependency can be described by linear functions. The slope and the *y*-intercept of these linear functions represents characteristic quantities. The slope describes the intensity of the increase of the heating rate due to an increase of the FVC. The *y*-intercept describes the extent of the contact area within a fabric layer if no compaction force is applied. It is shown that the increase of the heating rate due to an increase of the FVC is dominated by the used CF fabric. The higher the number of crossovers the higher the *y*-intercept and consequently the higher the heating rates at low FVC. The higher the slope the higher the influence of the compaction forces on the resultant contact area and consequently on the heating rate. Furthermore, it was showed that an increase of the thread-count leads to a lower slope and to a lower *y*-intercept. As the thread-counts increases, consequently the area weight of the fabric increases and the width of the rovings decreases. Hence, the resultant contact area and the applied compaction forces are smaller compared to a laminate made of a fabric with a low thread-count.

Acknowledgments

This work has been conducted in the frame of the project "Process Optimization of Induction Welding of Continuous Carbon-Fiber Reinforced Thermoplastics by Process Simulation" which is funded by the Deutsche Forschungsgemeinschaft (DFG, German Research Foundation) – MI 647/27-1.

References

[1] J. Border and R. Salas. Induction Heated Joining of Thermoplastic Composites Without Metal Susceptors. *34th International SAMPE Symposium and Exhibition, Covina, USA*, 1989.
[2] S. Becker and P. Mitschang. Influences of Textile Parameters on the Induction Heating behavior of CFRPC. *21st International Conference in Composite Materials, Xi'an, China*, 20-25th August 2017.